Asymmetric Magnetic Reconnection and Plasma Heating During Coronal Mass Ejections

Nick Murphy

Harvard-Smithsonian Center for Astrophysics

SSC Seminar
University of New Hampshire
November 3, 2010

Collaborators: John Raymond, Kelly Korreck, Carl Sovinec, Paul Cassak, Jun Lin, Chengcai Shen, & Aleida Young

Outline

- Asymmetric reconnection in CME current sheets
  - A scaling analysis of asymmetric outflow reconnection
  - Simulations of X-line retreat
  - Deriving an expression for X-line motion
- Plasma heating during the 28 June 2000 CME
  - Observations (UVCS, LASCO, EIT, MLSO/MK4, *GOES*)
  - Constraining heating with a time-dependent ionization code
  - Candidate mechanisms and connections with the laboratory

Introduction

- Magnetic reconnection, or the breaking and rejoining of magnetic field lines in a highly conducting plasma, occurs frequently in space, astrophysical, and laboratory plasmas
- Reconnection in physically realistic scenarios will often have asymmetry in the outflow direction
  - Current sheets behind coronal mass ejections (CMEs)
  - Earth's magnetotail
  - Spheromak merging experiments
  - Reconnection during plasma turbulence
- Often, outflow from one jet will propagate into a higher pressure region than the other jet
  - This then feeds back on local dynamics in the current sheet
- Such asymmetry determines where the energy goes
- *Definition*: An X-line is the line along which oppositely directed components of the magnetic field reconnect

Many models of CMEs predict a current sheet behind the rising flux rope (e.g., Lin & Forbes 2000)

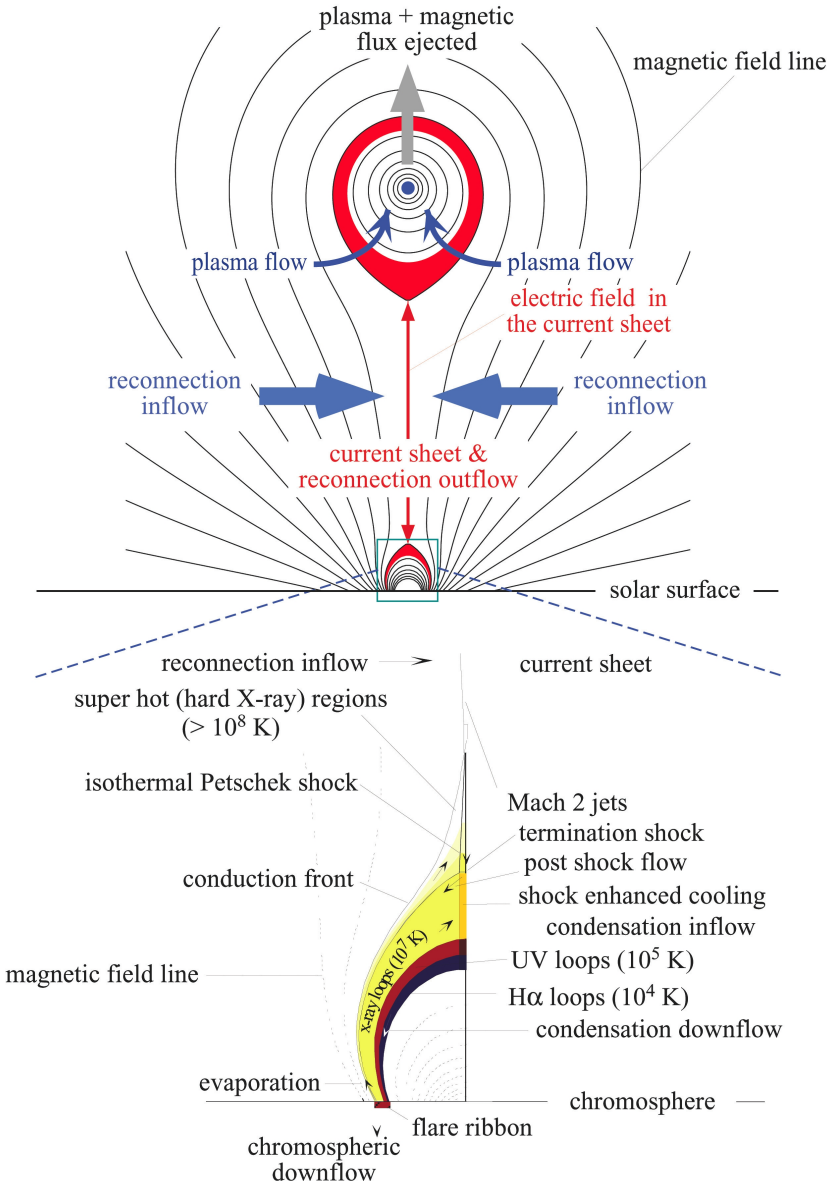

Current sheets behind CMEs have been observed for a number of events

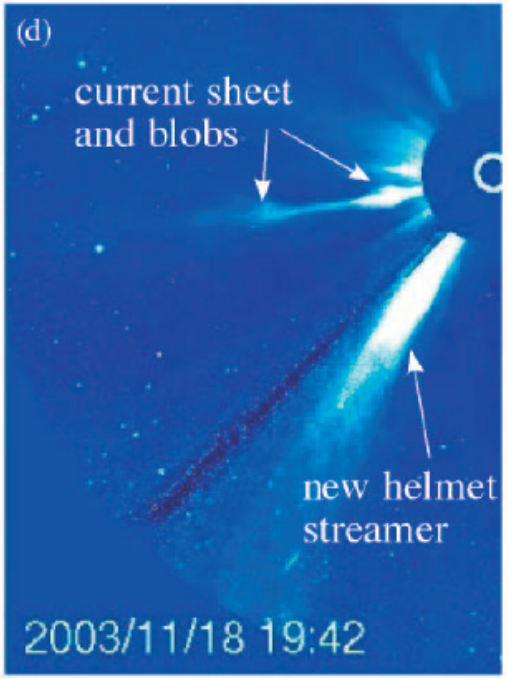

- Current sheets behind CMEs have been observed for a number of events (e.g., Ko *et al.* 2003; Lin *et al.* 2005; Ciaravella & Raymond 2008; Savage *et al.* 2010)
- Outward-moving blobs could be the result of the tearing or plasmoid instability in the current sheet (e.g., Lin *et al.* 2007)

Is reconnection in CME current sheets symmetric?

- Sunward outflow impacts a region of high plasma and magnetic pressure
- Antisunward outflow encounters the rising flux rope
- The upstream magnetic field strength and density are both strong functions of height
- Seaton (2008) predicts that the majority of the outflow is directed upward towards the rising flux rope, and that the flow stagnation point and magnetic field null should be near the base of the current sheet
- Savage *et al.* (2010) track upflowing (downflowing) features above (below) $h \sim 0.25 R_\odot$ in the 9 April 2008 'Cartwheel' CME current sheet. This is near the X-line in pre-event magnetic field models.

X-line motion is frequently observed in the magnetotail

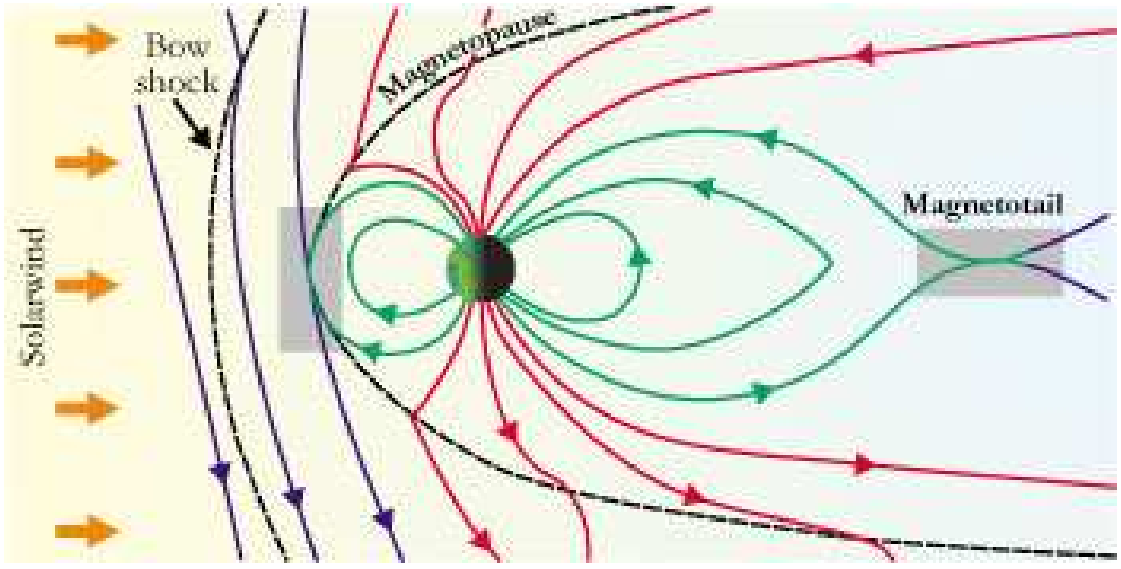

- The X-line is frequently observed to move tailward during the recovery phase of magnetospheric substorms
- Despite the prevalence of X-line retreat, it is standard practice to compare *in situ* measurements to particle-in-cell simulations of stationary reconnection layers

Murphy, Sovinec, & Cassak (2010) developed a scaling model for asymmetric outflow reconnection

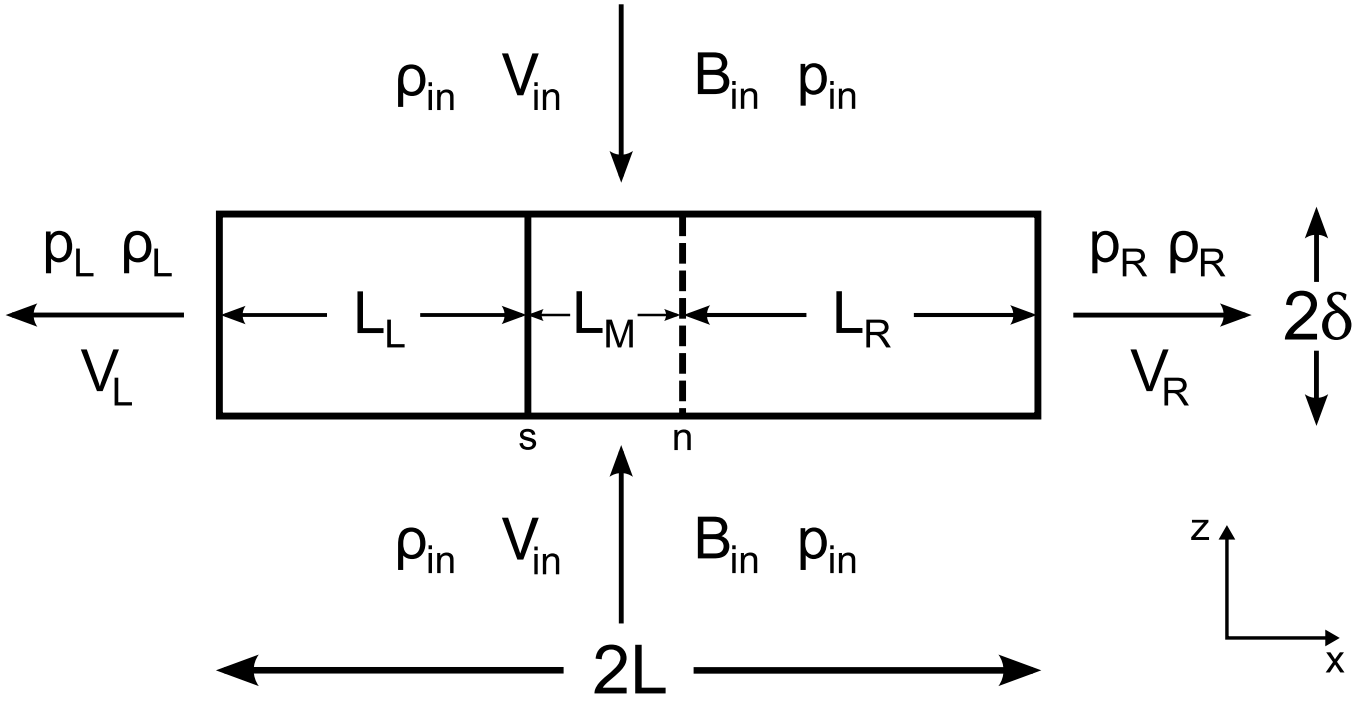

- The above figure represents a long and thin reconnection layer with asymmetric downstream pressure. Reconnection is assumed to be steady in an inertial reference frame.
- 'n' denotes the magnetic field null and 's' denotes the flow stagnation point

Scaling relations for asymmetric outflow reconnection

- Following Cassak & Shay (2007), we integrate over this control volume and find relations approximating conservation of mass, momentum, and energy

$$
\begin{aligned}
2\rho_{in} V_{in} L &\sim \rho_L V_L \delta + \rho_R V_R \delta \\
\rho_L V_L^2 + p_L &\sim \rho_R V_R^2 + p_R \\
2 V_{in} L \left(\alpha p_{in} + \frac{B_{in}^2}{\mu_0} \right) &\sim V_L \delta \left(\alpha p_L + \frac{\rho_L V_L^2}{2} \right) \\
&\quad + V_R \delta \left(\alpha p_R + \frac{\rho_R V_R^2}{2} \right)
\end{aligned}
$$

where $\alpha \equiv \gamma/(\gamma - 1)$ and we ignore upstream kinetic energy/downstream kinetic energy and assume the contribution from tension along the boundary is small or even.

Deriving the outflow velocity and reconnection rate

- In the incompressible limit

$$V_{L,R}^2 \sim \sqrt{4\left(c_{in}^2 - \frac{\bar{p}}{\rho}\right)^2 + \left(\frac{\Delta p}{2\rho}\right)^2} \pm \frac{\Delta p}{2\rho}$$

  using $\bar{p} \equiv \frac{p_L + p_R}{2}$, $\Delta p \equiv p_R - p_L$, and $c_{in}^2 = \frac{B_{in}^2}{\mu_0 \rho_{in}} + \frac{\alpha p_{in}}{\rho_{in}}$

- By assuming resistive dissipation, the electric field is then given by

$$E_y \sim B_{in}\sqrt{\frac{\eta\left(V_L + V_R\right)}{2\mu_0 L}}$$

Implications of scaling model

- The scaling relations show that the reconnection rate is weakly sensitive to asymmetric downstream pressure
  - If one outflow jet is blocked, reconnection is almost as quick
  - Reconnection slows down greatly only if both outflow jets are blocked
  - The current sheet responds to asymmetric downstream pressure by changing its thickness or length
- However, this analysis makes three major assumptions:
  - The current sheet is stationary
  - The current sheet thickness is uniform
  - Magnetic tension contributes symmetrically along the boundaries
- To make further progress, we must do numerical simulations

NIMROD solves the equations of extended MHD using a finite element formulation (Sovinec *et al.* 2004)

- In dimensionless form, the equations used for these simulations are

$$\frac{\partial \mathbf{B}}{\partial t} = -\nabla \times (\eta \mathbf{J} - \mathbf{V} \times \mathbf{B}) + \kappa_{divb} \nabla \nabla \cdot \mathbf{B} \tag{1}$$

$$\mathbf{J} = \nabla \times \mathbf{B} \tag{2}$$

$$\nabla \cdot \mathbf{B} = 0 \tag{3}$$

$$\rho \left(\frac{\partial \mathbf{V}}{\partial t} + \mathbf{V} \cdot \nabla \mathbf{V} \right) = \mathbf{J} \times \mathbf{B} - \nabla p - \nabla \cdot \rho \nu \nabla \mathbf{V} \tag{4}$$

$$\frac{\partial \rho}{\partial t} + \nabla \cdot (\rho \mathbf{V}) = \nabla \cdot D \nabla \rho \tag{5}$$

$$\frac{\rho}{\gamma - 1} \left(\frac{\partial T}{\partial t} + \mathbf{V} \cdot \nabla T \right) = -\frac{p}{2} \nabla \cdot \mathbf{V} - \nabla \cdot \mathbf{q} + Q \tag{6}$$

- Divergence cleaning is used to prevent the accumulation of divergence error

We perform resistive MHD simulations of two initial X-lines which retreat from each other as reconnection develops (see Murphy, Phys. Plasmas, 2010)

- The 2-D simulations start from a periodic Harris sheet which is perturbed at two nearby locations ($x = \pm 1$)
- Domain: $-30 \leq x \leq 30$, $-12 \leq z \leq 12$
- Simulation parameters: $\eta = 10^{-3}$, $\beta_\infty = 1$, $\mathrm{S} = 10^3$–10^4, $\mathrm{Pm} = 1$, $\gamma = 5/3$, $\delta_0 = 0.1$
- Define:
  - x_n is the position of the X-line
  - x_s is the position of the flow stagnation point
  - $V_x(x_n)$ is the velocity *at* the X-line
  - $\frac{\mathrm{d}x_n}{\mathrm{d}t}$ is the velocity *of* the X-line
- $\hat{\mathbf{x}}$ is the outflow direction, $\hat{\mathbf{y}}$ is the out-of-plane direction, and $\hat{\mathbf{z}}$ is the inflow direction
- We show only $x \geq 0$ since the simulation is symmetric

The current sheets have characteristic single wedge shapes

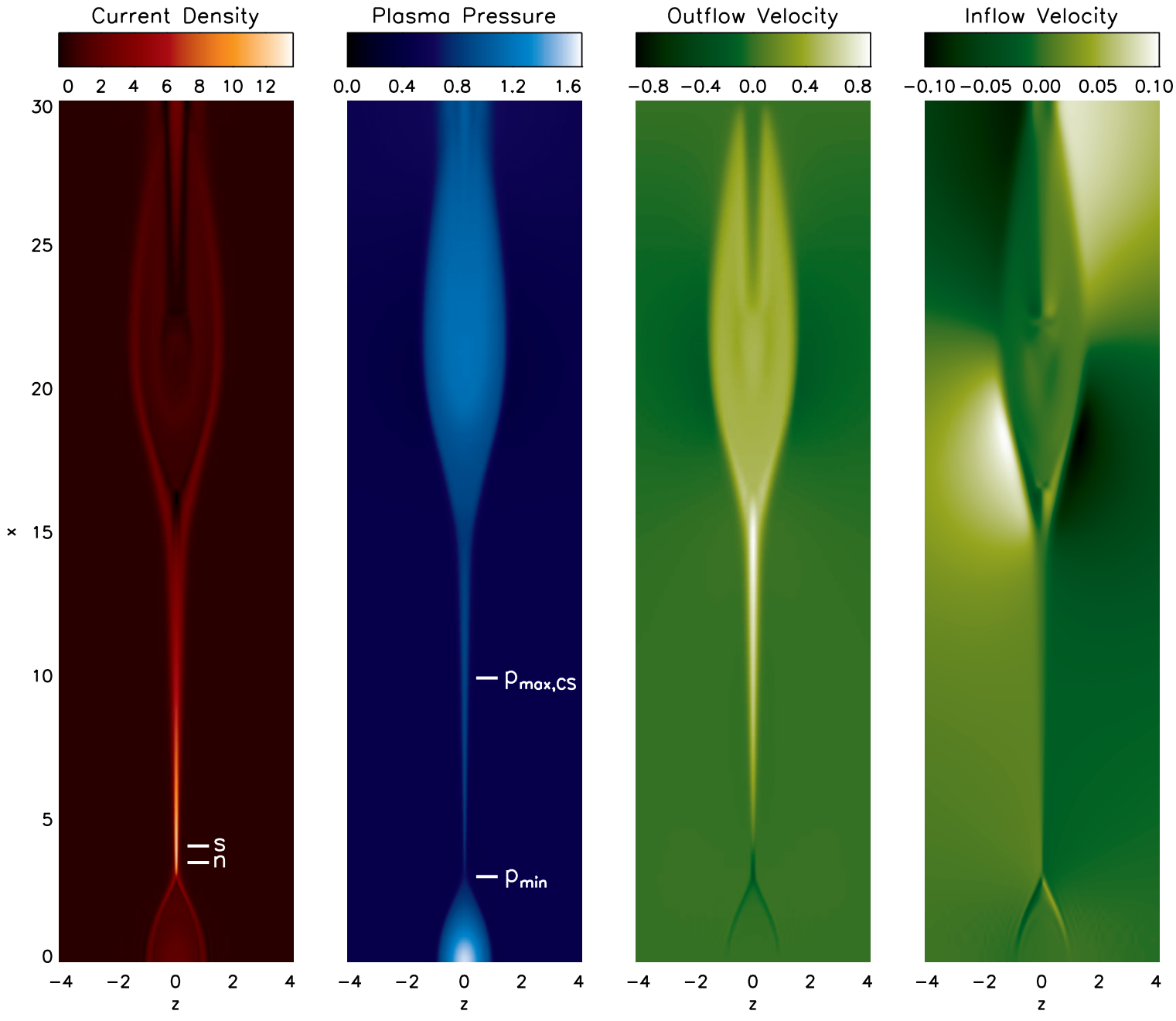

The outflow away from the obstruction is much faster

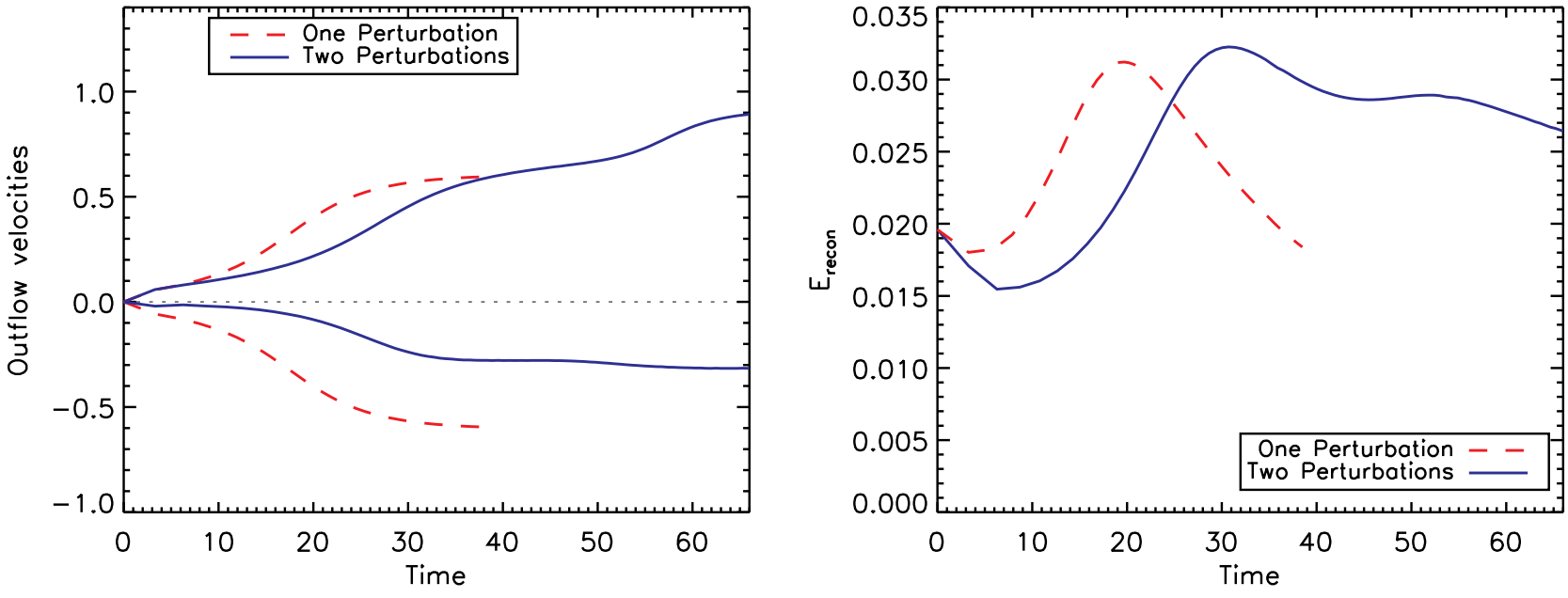

- In agreement with Seaton (2008) and Reeves *et al.* (2010), most of the energy goes away from the obstructed exit
- Eventually, reconnection is quicker in retreat simulations than in otherwise equivalent symmetric, non-retreating simulations
- The comparison with the symmetric case is halted at $t \approx 40$ because an island forms at $x = 0$

The flow stagnation point and X-line are not colocated

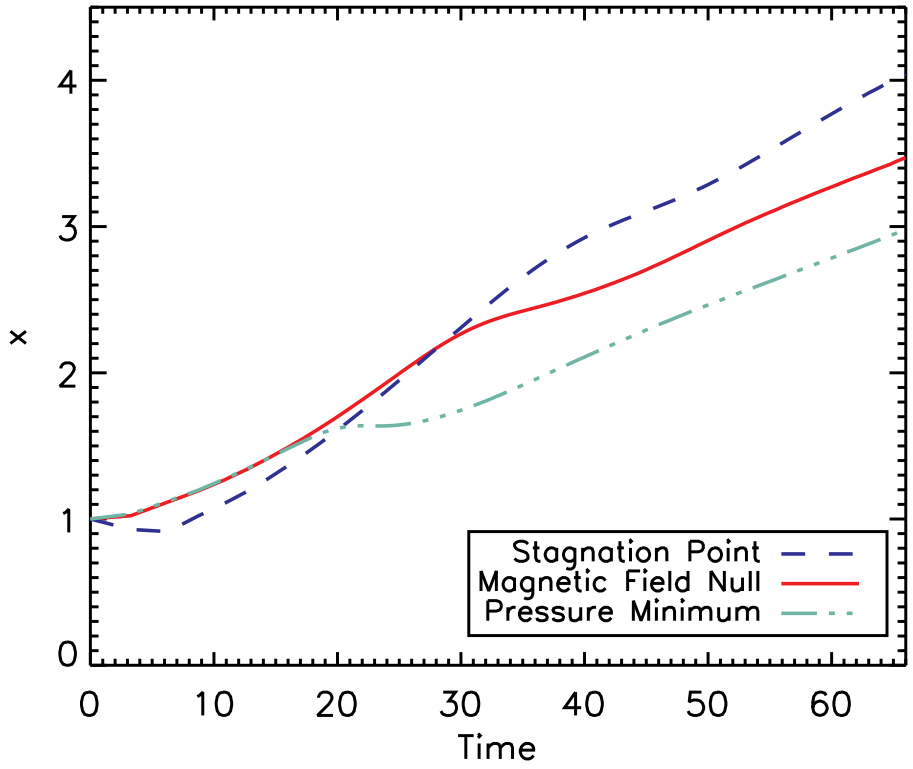

- Surprisingly, the relative positions of the X-line and flow stagnation point switch!
- This occurs so that the stagnation point will be located near where the tension and pressure forces cancel
- Reconnection develops slowly because the X-line is located near a pressure minimum early in time

Late in time, the X-line diffuses against strong plasma flow

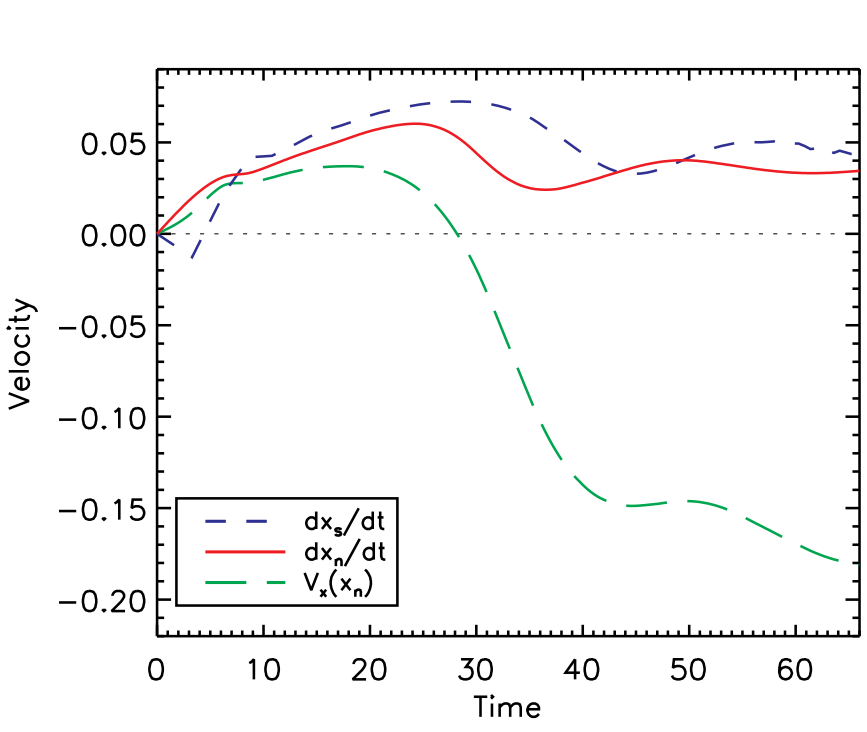

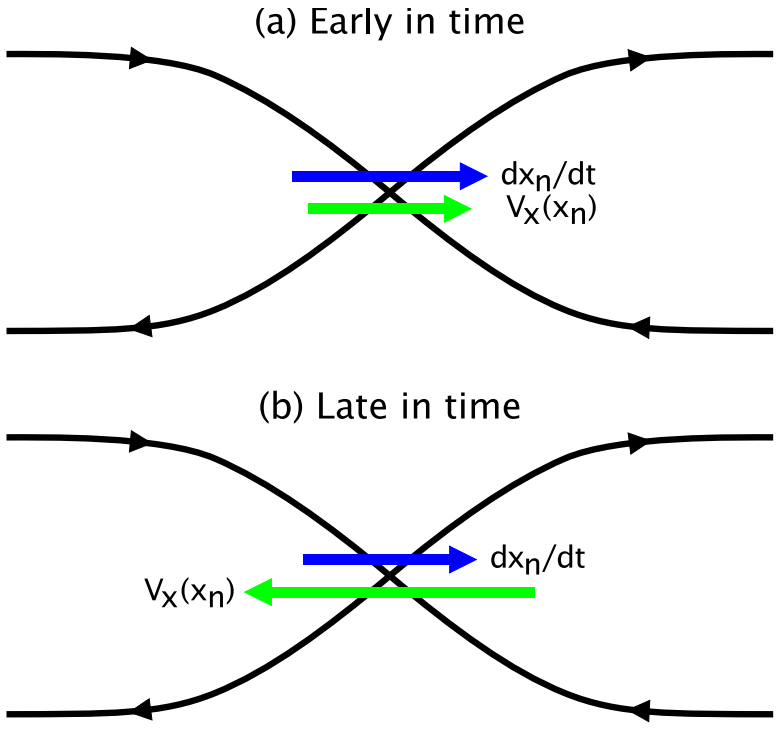

- The stagnation point retreats more quickly than the X-line
- Any difference between $\frac{\mathrm{d}x_n}{\mathrm{d}t}$ and $V_x(x_n)$ must be due to diffusion (e.g., Seaton 2008)
- The velocity *at* the X-line is not the velocity *of* the X-line

What sets the rate of X-line retreat?

- The inflow (z) component of Faraday's law for the 2D symmetric inflow case is

$$\frac{\partial B_z}{\partial t} = -\frac{\partial E_y}{\partial x} \tag{7}$$

- The convective derivative of B_z at the X-line taken at the velocity of X-line retreat, $\mathrm{d}x_n/\mathrm{d}t$, is

$$\left.\frac{\partial B_z}{\partial t}\right|_{x_n} + \frac{\mathrm{d}x_n}{\mathrm{d}t}\left.\frac{\partial B_z}{\partial x}\right|_{x_n} = 0 \tag{8}$$

The RHS of Eq. (8) is zero because $B_z(x_n, z = 0) = 0$ by definition for this geometry.

Deriving an expression for X-line retreat

- From Eqs. 7 and 8:

$$\frac{\mathrm{d}x_n}{\mathrm{d}t} = \left.\frac{\partial E_y/\partial x}{\partial B_z/\partial x}\right|_{x_n} \tag{9}$$

- Using $\mathbf{E} + \mathbf{V} \times \mathbf{B} = \eta \mathbf{J}$, we arrive at

$$\frac{\mathrm{d}x_n}{\mathrm{d}t} = V_x(x_n) - \eta \left[\frac{\frac{\partial^2 B_z}{\partial x^2} + \frac{\partial^2 B_z}{\partial z^2}}{\frac{\partial B_z}{\partial x}}\right]_{x_n} \tag{10}$$

- In the simulations $\frac{\partial^2 B_z}{\partial z^2} \gg \frac{\partial^2 B_z}{\partial x^2}$, so X-line retreat is caused by diffusion of the normal component of the magnetic field along the inflow direction
- Equation (9) can also be evaluated using additional terms in the generalized Ohm's law

Mechanism and implications

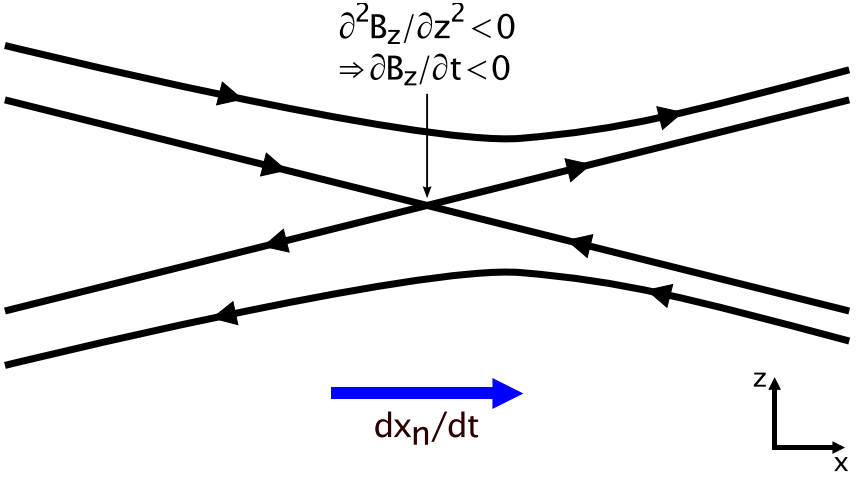

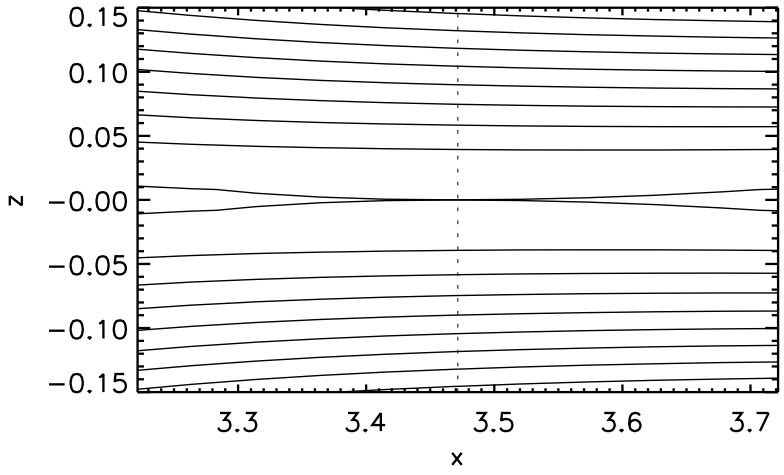

- The X-line moves in the direction of increasing total reconnection electric field strength
- X-line retreat occurs through a combination of advection by bulk plasma flow and diffusion of the normal component of the magnetic field
- X-line motion depends intrinsically on local parameters evaluated at the X-line

Asymmetric outflow reconnection may have implications for two important observed properties of CMEs

- The masses of CMEs are known to increase with time during their early evolution
  - Bemporad *et al.* (2007) presented one event where $\sim 2/3$ of the CME mass originates above $1.6 R_{\odot}$
  - Vourlidas *et al.* (2010) show that the final mass of CMEs is set around $\sim 10 R_{\odot}$
- CMEs continue to be heated even after the ejecta leaves the flare site
  - Some heating mechanism must counter adiabatic cooling
  - See Akmal *et al.* 2001; Ciaravella *et al.* 2001; Lee *et al.* 2009; Landi *et al.* 2010; Murphy *et al.*, in prep
- Outflow from the CME current sheet may explain both of these properties (e.g., Lin *et al.* 2004)
- Next, we consider evidence for CME heating during one event and discuss additional candidate heating mechanisms

On 28 June 2000, a fast and powerful CME was observed by *SOHO*/UVCS

- *SOHO*/EIT 195 Å observations show a rising dark arcade between 18:00–18:48
- *GOES* observed a C3.7 class X-ray flare starting at 18:48 UT
  - The footpoints may have been behind the limb so the flare might have been partially occulted
- While light coronagraph observations by the Mauna Loa Solar Observatory (MLSO) show possible kinking of the rising flux rope
- Ciaravella *et al.* (2005) use UVCS and LASCO measurements to detect a coronal shock wave driven by this event
- A fast, powerful CME with an apparently weak flare

SOHO/EIT observations show a rising dark arcade at 195 Å followed by bright He II arches at 304 Å

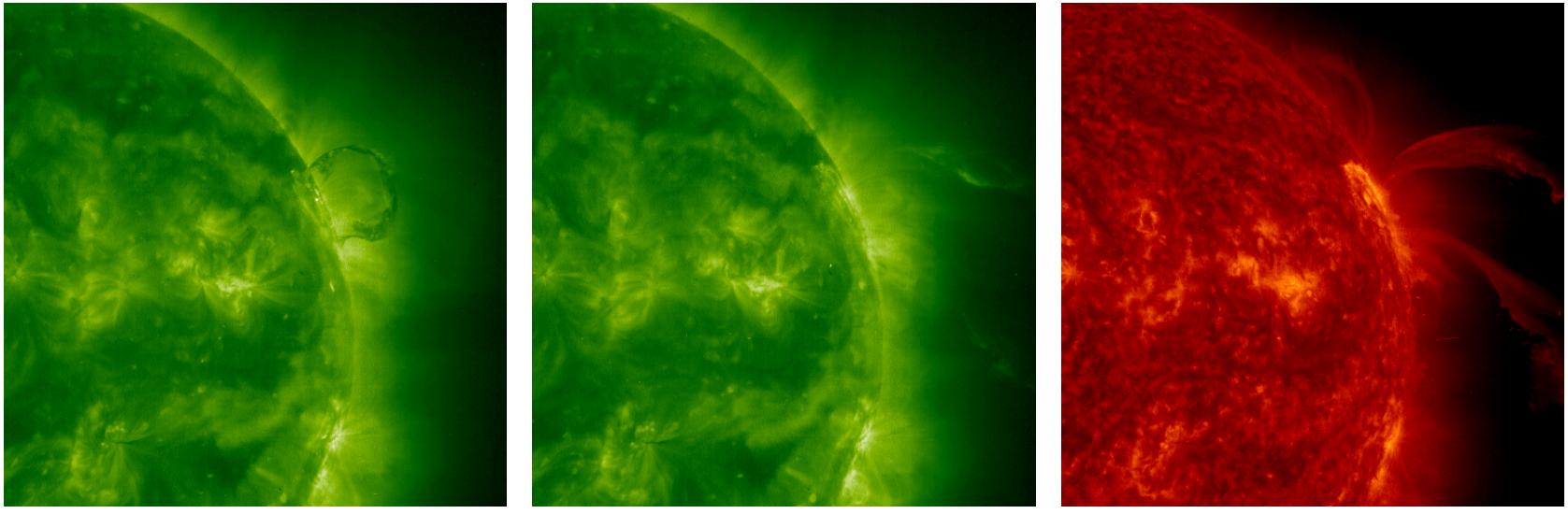

- *From left to right:* 195 Å at 18:48 UT and 19:13 UT, and 304 Å at 19:19 UT

SOHO/LASCO observations show the rising prominence crossing the UVCS slit

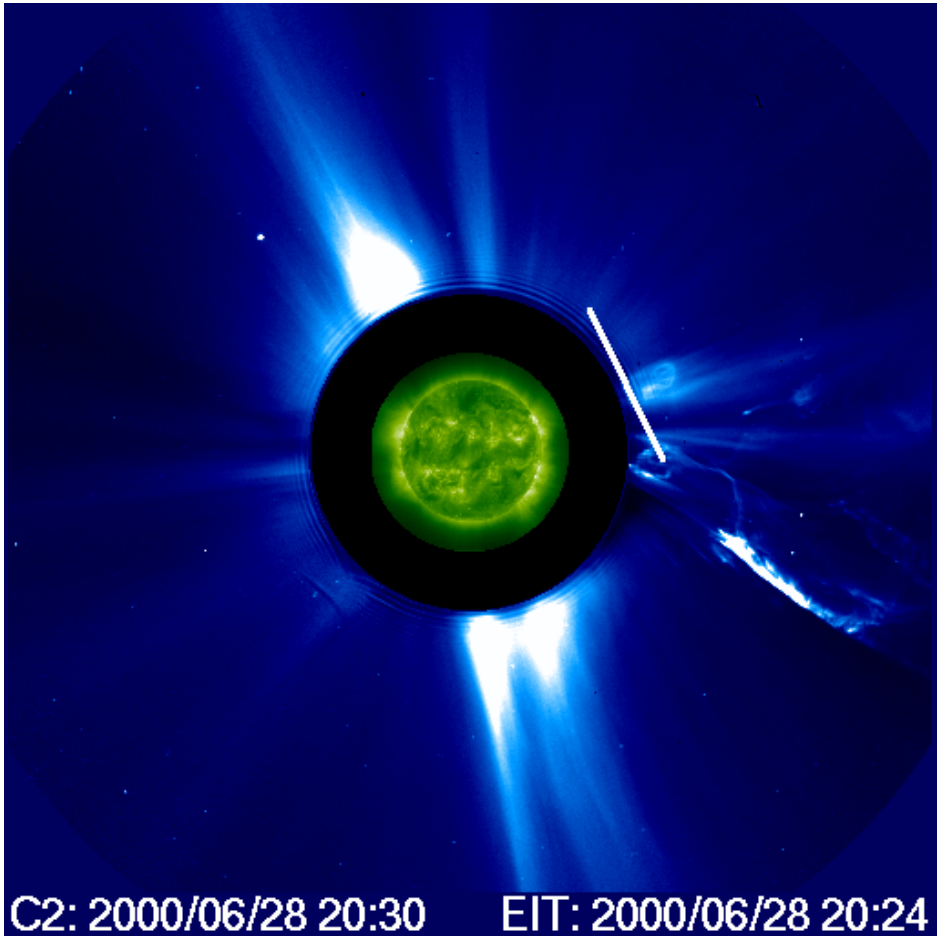

- We consider in detail one particular feature with good constraints on the heating rate: the rising prominence

We use a 1-D time-dependent ionization code to track ejecta between the flare site and UVCS slit

- We run a grid of models with different initial densities, initial temperatures, and heating rates (e.g, Akmal *et al.* 2001)
- The final density is derived from UVCS observations
  - The density sensitive [O V]/O V] line ratio
  - Radiative pumping of the O VI doublet
- Assume homologous expansion
- Multiple heating parameterizations
  - An exponential wave heating model by Allen *et al.* (1998)
  - The expanding flux rope model by Kumar & Rust (1996)
  - Heating proportional to n or n^2
- Velocities are scaled from Maričić *et al.* (2006)
- The models consistent with UVCS observations give the allowable range of heating rates

UVCS observations show a diagonal feature in O V and O VI at 20:11 UT

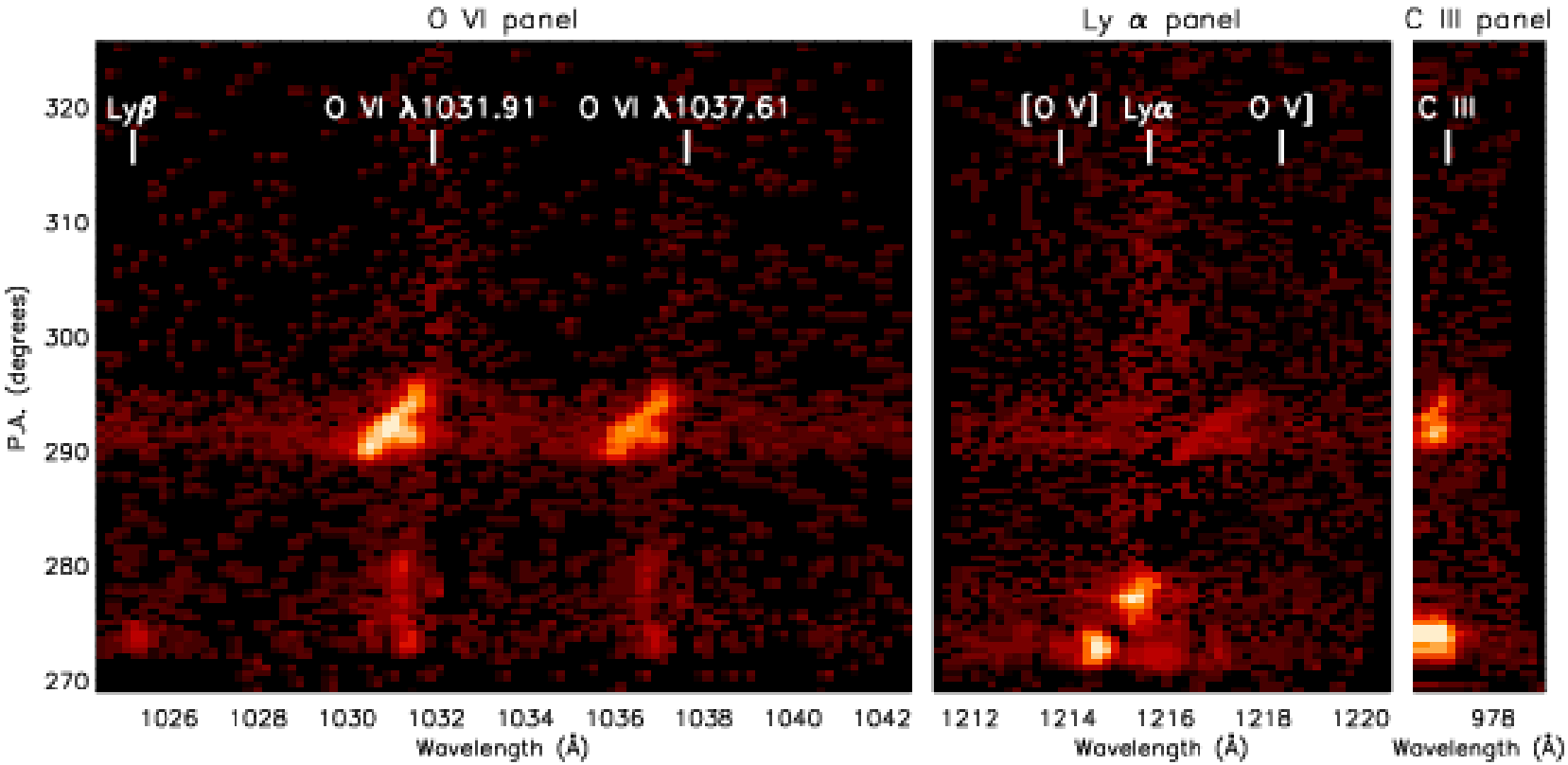

- Observed lines include O V, O VI, Lyα, Ly β, C II, C III, N III
- This diagonal shear flow feature is consistent with an expanding flux rope observed at an angle to the line of sight

Weak Lyα in this feature allows both [O V] and O V] to be observed

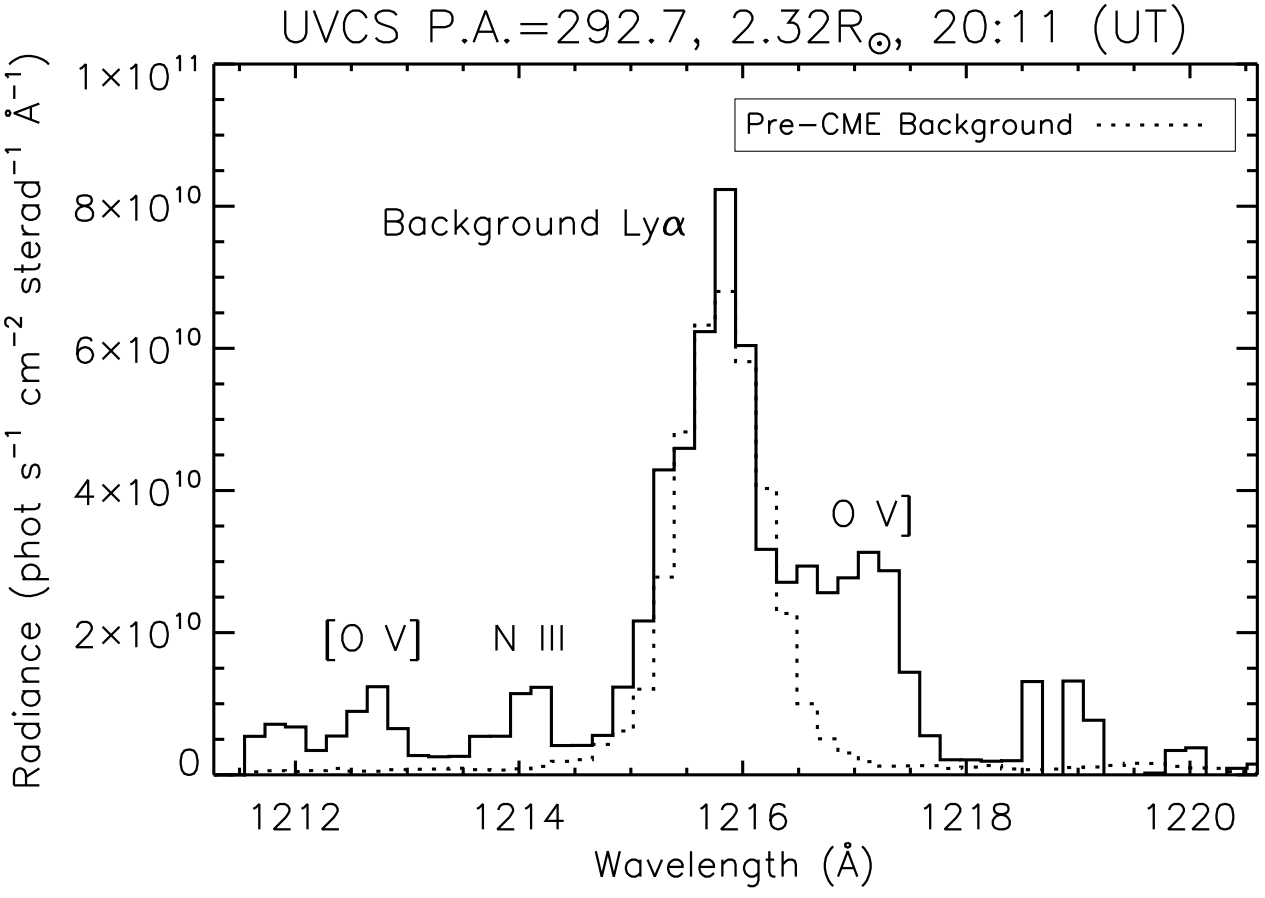

- The N III $\lambda\lambda 989, 991$ lines sometimes appear at the same position on the detector as [O V] at 1213.9 Å

Caveats and considerations

- Observations are averaged across the line of sight
  - UVCS may be observing multiple components at different temperatures simultaneously
  - We assume that O V and O VI emission is from the same plasma, and take Lyα, C II, C III, and N III emission as upper limits
- Some heating parameterizations are not amenable to a 1-D analysis
  - Reconnection outflow from the CME current sheet
  - Kink-like motions driving waves which then dissipate
- No physical heating mechanism is assumed, except for the wave heating model

The total heating is greater or comparable to the kinetic energy of the ejecta

- In this feature associated with the rising prominence, the total heating is $\sim$1.8–12 eV/proton
- The kinetic energy is $\approx$1.1–1.4 eV/proton
- Total heating $\gtrsim$ kinetic energy
- Coronal magnetic fields are difficult to diagnose so their contribution to the energy budget is uncertain (but large)
- The results of this and previous analyses suggest that CME models should take plasma heating into account
- However, the heating mechanism is not understood

Candidate heating mechanisms include:

- Reconnection outflow from the CME current sheet
  - Recent theoretical/numerical results suggest that most of the energy goes away from the Sun
- Wave heating from photospheric motions
  - Landi *et al.* (2010) show that heating $\sim$1500 times that of coronal holes would be needed for the 'Cartwheel CME'
- The kink instability of the expanding flux rope
  - But, $V_{\rm kink} < V_{\rm CME}$
- Magnetic dissipation/the tearing instability
- Thermal conduction/energetic particles from flare
  - Unlikely because a C class flare is associated with this event

Connections with laboratory plasma experiments

- Tripathi and Gekelman (2010) showed that an erupting flux rope generates intense magnetosonic waves which heat the ambient plasma
- Asymmetric outflow reconnection occurs in spheromak merging experiments (MRX, SSX, TS-3/4)
- Potentially relevant flux rope experiments are performed at MRX, RSX, LAPD, the Caltech spheromak experiment, and elsewhere

Conclusions

- X-line motion occurs frequently during magnetic reconnection in space, astrophysics, and the laboratory
- Resistve MHD simulations of X-line retreat show significant flow across the X-line in the opposite direction of X-line retreat
- An expression for the rate of X-line retreat shows that X-line motion is due to either advection by the bulk plasma flow or by diffusion of the normal component of the magnetic field
- Heating is an important but poorly understood term in the energy budget of CMEs
- Candidate CME heating mechanisms include
  - Upflow from the CME current sheet
  - Large-scale MHD instability of the expanding flux rope
  - Thermal conduction/energetic particles from the flare
  - Dissipation of MHD waves/turbulence

Future work

- X-line retreat
  - Extend simulations to include two-fluid or 3-D effects
  - Generalize the expression for X-line retreat to include additional terms in the Ohm's law and 3-D geometry
  - Investigate X-line motion in asymmetric inflow reconnection
  - Examine X-line dynamics during the plasmoid instability
  - Look for signatures of asymmetric outflow reconnection in CMEs and the Earth's magnetotail
- The energy budget of CMEs
  - Perform a standardized time-dependent ionization analysis for $\sim$10–20 CMEs to allow comparisons between different events
  - Use theory or simulation to better predict how each heating mechanism behaves
  - Use these results to constrain or rule out candidate heating mechanisms